

Interplay between spin and phonon fluctuations in the double-exchange model for the manganites

Massimo Capone

Dipartimento di Fisica, Università di Roma "La Sapienza," and Istituto Nazionale per la Fisica della Materia (INFM), Unità Roma 1, Piazzale Aldo Moro 2, I-00185 Roma, Italy

Sergio Ciuchi

Dipartimento di Fisica, Università de L'Aquila, and Istituto Nazionale per la Fisica della Materia (INFM), Unità de L'Aquila, Via Vetoio, I-67100 L'Aquila, Italy

(Received 3 July 2001; revised manuscript received 27 September 2001; published 12 February 2002)

We present exact solutions, mainly analytical, for the two-site double-exchange-Holstein model, that allow us to draw a complete picture of the role of both phonon and spin quantum fluctuations in determining the short-range correlations in the manganites. We provide analytical solutions of the model for arbitrary electron-phonon coupling and phonon frequency, for $S=1/2$ and for the classical spin limit $S=\infty$, and compare these results with numerical diagonalization of the realistic $S=3/2$ case. The comparison reveals that the realistic case $S=3/2$ is not well described by the classical spin limit, which is often used in literature. On the other hand, the phonon fluctuations, parametrized by the phonon frequency ω_0 , stabilize ferromagnetic phases with respect to the adiabatic limit. We also provide a complete analysis on the polaron crossover in this model.

DOI: 10.1103/PhysRevB.65.104409

PACS number(s): 75.50.Dd, 75.50.Ee, 71.38.Ht

I. INTRODUCTION

It is known from the 1950's that the double exchange mechanism¹⁻³ is at the basis of the magnetic properties of the manganese perovskites $R_{1-x}A_x\text{MnO}_3$ [where R is a rare earth element (e.g., La), and A is a divalent element such as Sr or Ca]. In this compounds, the d levels of each Mn ion host $4-x$ electrons. Three of them occupy the three low-lying t_{2g} levels, with aligned spins due to the Hund's rule. These electrons are basically localized, and only the $1-x$ electrons in the e_g level contribute to the transport properties. The discovery of the so-called "colossal" magnetoresistance⁴ has originated an enormous revival of studies on these compounds, both on the theoretical and the experimental side. The systematic experimental investigations of the last few years have underlined some weakness in the previous understanding, unveiling a surprisingly rich phase diagram where a lot of competing phases are stabilized by varying doping, temperature and chemical nature of the dopants. One of the most relevant new theoretical trends is the suggestion that the transport properties cannot be fully understood on the basis of the double exchange alone, and that the interplay of this mechanism and a significant electron-phonon (e -ph) interaction leading to a Jahn-Teller (JT) effect is the key for the explanation of these properties.⁵ The preeminent role of e -ph effects has also been firmly established experimentally by various groups and techniques.⁶

The complex entanglement between charge, orbital, and lattice degrees of freedom represents a hard theoretical challenge, that is far from being solved. Many approximate solutions and numerical results have been proposed, but the complexity of the phase diagram has naturally forced various authors to many uncontrolled simplifications. In this work we make a step back, and focus on a system for which *analytical* exact results can be obtained. Namely, we solve the double exchange model for a single electron on two sites in

the presence of a local Holstein e -ph coupling.⁷ Since we are interested in the relevant physics determining the interplay between lattice and spin quantum fluctuations, we consider the simple Holstein model, instead of a more involved Jahn-Teller coupling. This choice does not imply a loss of generality since we are not discussing the role of orbital degrees of freedom.

The two-site system has been extensively studied as the minimal system able to capture the key features of polaron formation from the point of view of ground state⁸⁻¹¹ as well as spectral properties.^{12,13} Recently also the interplay between e -ph and e - e correlations has been studied semianalytically within the same model.¹⁴ However, as far as magnetic properties are concerned, it is quite obvious that a two-site system does not allow for long-range order and phase transitions. Nevertheless, it shows *short-range* (nearest neighbors) correlations, that give substantial indications on the actual long-range properties of the system, at least in strong coupling. In the context of the models for the manganites it is in fact believed that the finite-size effects play a little role.¹⁵ We will discuss the relevance of our results to large systems in the following.

Due to the simplicity of the model, we can give complete exact phase diagrams without approximations. One of our main results is a complete characterization of the role of the quantum fluctuations of the core t_{2g} spins. In a microscopic model of the manganites, the core spins have $S=3/2$, and this value is usually thought to be large enough to get rid of quantum fluctuations and treat them as classical variables. We will explicitly test this assumption by comparing the limiting cases $S=\infty$ (classical spins) and the extreme quantum case $S=1/2$, where the effect of quantum fluctuations is maximum, with the realistic $S=3/2$ case.

Analogously, we will discuss the role of lattice quantum fluctuations, releasing the adiabatic approximation on the phonon degrees of freedom. The role of quantum phonon fluctuations is not trivial, as already known for e -ph models alone.¹⁶⁻¹⁸ For $S=\infty$ and $S=1/2$ we give analytical exact

solutions of the model, exploiting an exact analytical solution of the two-site Holstein model. For $S=3/2$ we use standard exact diagonalization to solve the model. Also in this case no approximation is introduced and all the regimes are accessible.

A similar study has been reported in Ref. 19, where the two-site double exchange model for *classical spins* is solved by perturbation theory around a variational reference state obtained by a Lang Firsov canonical transformation. Our work overcomes some limitations of Ref. 19, namely the classical spin limit. Contrary to Ref. 19, we are also able to explore the adiabatic regime $\omega_0 \ll t$, well beyond the region in which the Lang Firsov result is a good reference state.

The paper is organized as follows: In Sec. II we introduce the model and the methods for our analytical solutions. In Sec. III we present the phase diagram of the model and discuss the role of quantum fluctuations; due to the complexity of the phase diagram the discussion is divided in three subsections: in the first the effect of the magnetic degrees of freedom on the polaron crossover is considered; in the second we discuss the effect of the e -ph interaction on the magnetic phase diagram of the model, and in the third subsection the full phase diagram is presented.

In Sec. IV we discuss the relevance of our results for larger size systems and for the experimental scenario. Finally we give concluding remarks in Sec. V.

II. METHODS OF SOLUTION

We consider the Holstein double exchange model on a two-site cluster for a single electron

$$H = -t \sum_{\sigma} (c_{1,\sigma}^{\dagger} c_{2,\sigma} + c_{2,\sigma}^{\dagger} c_{1,\sigma}) - J_H \sum_{i=1,2} \boldsymbol{\sigma}_i \cdot \mathbf{S}_i + J_1 \mathbf{S}_1 \cdot \mathbf{S}_2 - g(n_1 - n_2)(a + a^{\dagger}) + \omega_0 a^{\dagger} a, \quad (1)$$

where \mathbf{S}_i ($i=1,2$) is a local spin associated to the localized t_{2g} electrons on each site, $c_{i,\sigma} (c_{i,\sigma}^{\dagger})$ destroys (creates) an electron of spin σ on site i , $n_i = \sum_{\sigma} c_{i,\sigma}^{\dagger} c_{i,\sigma}$ is the number operator on each site, $\boldsymbol{\sigma}_i = c_{i\alpha}^{\dagger} \vec{\sigma}_{\alpha\beta} c_{i\beta}$ is the spin operator on each site ($\vec{\sigma}$ are the Pauli matrices). a (a^{\dagger}) is the destruction (creation) operator for a lattice distortion that couples to the difference of density between the two sites. The lattice displacement X is given by $X = \sqrt{\hbar/2m\omega_0}(a + a^{\dagger})$. We could have started from a standard Holstein model with a phonon mode per each site, coupled to the local density. It is in fact easy to show that, in this case, the symmetric combination of the two phonon modes $A = 1/\sqrt{2}(a_1 + a_2)$ couples to the total density, giving rise to a trivial term, and the only term left is the one we introduced, where the phonon mode may be written in terms of the local ones as $a = 1/\sqrt{2}(a_1 - a_2)$.

We explicitly consider, in addition to the hopping between the two sites and the Hund's rule term (J_H) that couples ferromagnetically the conduction electrons to the localized ones, an antiferromagnetic superexchange term (J_1) between the core electrons. J_H is always taken to be the largest energy scale, consistently with the physics of the manganites. This latter term, even though J_1 is significantly smaller than J_H ,

has crucial importance on the magnetic properties of the manganites.²⁰ We also consider a Holstein coupling (g) between the electron and a dispersionless mode of frequency ω_0 .

In this paper, we present the *exact* solution for the model (1). In particular for the classical spin case $S=\infty$ and the extreme quantum case $S=1/2$ we provide *analytical* solutions for arbitrary values of both the electron-phonon coupling and of the phonon frequency ω_0 , exploiting an exact solution of the two-site Holstein model reported in Appendix A. In the $S=3/2$ case, a numerically exact solution by means of exact diagonalization is instead presented. Despite the electronic Hilbert space is really small, the infinite phonon Hilbert space requires some truncation. As customary (see, e.g., Ref. 16), we allow for a maximum number of phonons n_{ph} per site and check for convergence as a function of this number. The values of n_{ph} for which convergence is achieved depend on the physical regime. Even in the strong coupling limit, and in the adiabatic regime, where a large number of phonons is present in the ground state, this number may be at most $n_{\text{ph}} \sim 100$, a number that can be easily handled with the Lanczos method. In the following subsections, we describe the analytical solutions for $S=1/2$ and $S=\infty$.

It is clear that a two-site system cannot undergo a true phase transition. Nevertheless this is the minimal model in which non local correlation functions can be defined. These correlation functions will help us in defining the nature of the ground state of the system. Quite obviously, changing the parameters of the Hamiltonian, the ground state will display different physics. In the following we will call these modifications "transitions," with slight abuse of language. Depending on the way in which the nature of the ground state of the system changes, we will distinguish between continuous and discontinuous "transitions." For a "discontinuous transition" we mean the level crossing between states having different quantum numbers resulting in a discontinuous change of the non local correlation function. On the other hand, we define as "continuous transition" (crossovers) the continuous change of the nature of the ground state without change of the quantum numbers.

A. Exact solution for $S=\infty$

Following Ref. 2, in the classical spins case we can write

$$H(\theta) = J_1 \cos \theta - H_H(\theta) + E_{\text{Hund}}, \quad (2)$$

where E_{Hund} is the contribution of the Hund's term to the total energy and H_H is the Hamiltonian of a two-site Holstein model in which the hopping t is replaced by $\bar{t} = t \cos(\theta/2)$. The canting angle θ , that measures the relative orientation of the core spins fully characterizes the magnetic arrangement. If $\theta=0$ the spins are aligned and a ferromagnetic (FE) state is found, whereas for $\theta=\pi$, an antiferromagnetic state (AF) is found. Intermediate values of θ describe canted (CA) states. Therefore, the solution of the classical spins two-sites Holstein double-exchange model can be obtained by minimizing on θ , once the eigenvalues of H_H are known, as shown in Appendix A. For $J_H \gg J_1$ the extremal condition then gives

$$\sin(\theta/2) \left(-2J_1 \cos(\theta/2) - \frac{t}{2} \frac{\partial E_H}{\partial \bar{t}} \right) = 0, \quad (3)$$

which shows that the ferromagnetic state $\theta=0$ is always an extremum of $E(\theta)$.²¹ Then the “transition” from FE to CA state is continuous. The critical coupling J_1 for this “transition” is given by the vanishing of the term in parentheses in Eq. (3)

$$J_1^c = \frac{-E_H^{\text{kin}}}{4}, \quad (4)$$

where $E_H^{\text{kin}} = t \partial E_H / \partial t$ is the kinetic energy of the Holstein model, i.e., the kinetic energy of the system with $J_1=0$ (Notice that E_H^{kin} is a negative quantity). The effect of e -ph interaction on the FE \rightarrow CA “transition” is therefore the substitution $t \rightarrow -E_{\text{kin}}$.

Now let us consider the discontinuous FE \rightarrow AF “transition.” We have to compare the FE and AF energies obtained by Eq. (2), respectively, with $\theta=0$ and $\theta=\pi$. The critical coupling is given by

$$J_1^c = \frac{E_H(0) - E_H(\pi)}{2}, \quad (5)$$

where $E_H(0) = -g^2/\omega_0$ is the energy of the atomic Holstein model.

B. Exact solution for $S=1/2$

In this case, neglecting for the moment the phonon degrees of freedom, the electronic Hilbert space (including the core spins) is in principle made by 16 states, that reduce to 8 if the symmetry for inversion of all the spins is considered. As shown in Appendix B, this problem can be simplified, and the largest subspace to deal with is a 3×3 sector, but the remaining problem is still not trivial if we switch on the coupling with the phonons. Fortunately, in the limit $J_H \gg t$, a further simplification occurs (also shown in Appendix B), leading to the possibility to express the eigenvalues of the model in terms of the two-site Holstein model. The details of the solution are reported in Appendix B. In such a way, we can characterize the condition for the only possible “transition,” i.e., the one from FE to AF ground state. The “transition” is discontinuous and can be obtained from the comparison of the energies of the different phases, that we compute in Appendix B. The critical coupling for the FE \rightarrow AF “transition” is then given by

$$J_1^c = \frac{4[E_H(t/2) - E_H(t)]}{3}, \quad (6)$$

where E_H is the energy of the two-site Holstein model. Contrary to the classical spin case quantum spin fluctuations allow for non zero effective hopping $\bar{t} = t/2$ in the AF phase.

III. RESULTS

In this section, we present the phase diagrams of the model (1), with a particular emphasis on the interplay be-

tween the role of phonon and spin quantum fluctuations (measured, respectively, by ω_0/t and the value of the “local” spin of the t_{2g} electrons S). Due to the relatively large number of parameters that determine the phase diagram, we organize the discussion of the results in subsections: in the first subsection we discuss the polaron crossover in the different regimes, providing a unifying picture of the effect of both phonon and spin fluctuations, and of electron-spin correlation, that generalizes in a consistent way the conditions for the small polaron crossover in the simplest Holstein model.^{16–18} In the second subsection, we discuss the magnetic “transitions” occurring in our model. Both the nature of the magnetic phases and the relation between the magnetic state and the occurrence of polaronic behavior are strongly dependent on the value of the spin S . Finally, in the last subsection, we present complete phase diagrams in the λ - J_1 plane, where the role of lattice and magnetic degrees of freedom is highlighted.

A. The polaron crossover

Models with electron-phonon interaction quite generally exhibit a polaronic ground state when the coupling strength is large enough. The transformation of the free electron into a small polaron is not a phase transition, but a continuous crossover. For the Holstein model and a single particle, it has been shown that the condition for the crossover significantly depends upon the ratio between the phonon frequency ω_0 and the typical electronic energy scale t . In the adiabatic regime $\omega_0 \ll t$, the crossover occurs for $\lambda = g^2/\omega_0 t \approx 1$, whereas in the antiadiabatic regime $\omega_0 \gg t$, the crossover is controlled by the (purely phononic) variable $\alpha = g/\omega_0$.^{16–18} As a matter of fact, the crossover coupling λ_{pol} is pushed to larger values of λ as the frequency is increased. Moreover, the crossover becomes smoother and smoother as ω_0/t gets larger.

The conditions for a polaron crossover in the adiabatic and antiadiabatic regimes can be understood on basic physical grounds. In the adiabatic regime, the key condition is that a bound state can be formed. The condition $\lambda > 1$ expresses this property, since it just implies that the polaron binding energy $E_{\text{pol}} = g^2/\omega_0$ exceeds the kinetic energy of a free electron $\sim t$. On the other hand, in the antiadiabatic limit, the electronic energy scale t is not the largest scale, and the polaron crossover is ruled by the condition $\alpha^2 > 1$, that corresponds to the excitation of a significant number of phonons (or, equivalently, to a sizable lattice distortion). The crossover conditions we have just described are based on simple, model independent, physical insights, and are therefore expected to basically hold, with some marginal changes, also for more complicated models such as the double-exchange model we are considering.

It must be noted that, since the formation of a polaron is not a phase transition with an associated broken symmetry, there is some ambiguity in determining a physically sensible clear-cut criterion for the polaron crossover. In most previous studies, including that of Ref. 19, the crossover line has been drawn as the locus of the points in which some relevant expectation values, such as the electron-lattice correlation

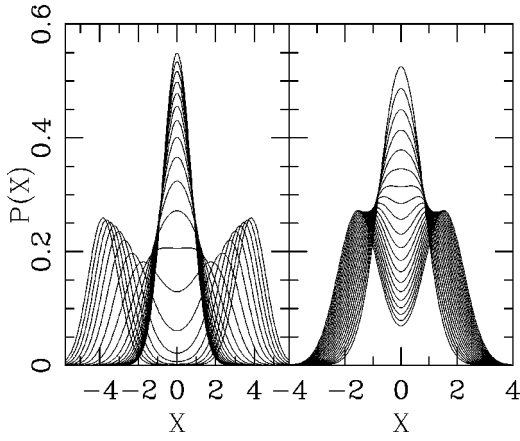


FIG. 1. Phonon displacement distribution function $P(X)$ for the two-site Holstein model for $\omega_0/t=0.1$ and $\omega_0/t=4$. The various lines in the two panels correspond to different values of λ . For $\omega_0/t=0.1$ λ ranges from 0 to 1.4, whereas for $\omega_0/t=4$ $0 < \lambda < 4$.

function $1/N \sum_i \langle n_i X_i \rangle$ or the average number of phonons in the ground state change their behavior. This kind of characterization has no problem in the adiabatic regime, where the crossover is rather sharp, but it is more questionable in the antiadiabatic regime. In this work we use a much more definite criterion, that is based on a *qualitative* difference between polaronic and nonpolaronic states. Namely, we study the (quantum) probability distribution function for the displacement operator $P(X) = \langle 0|X\rangle\langle X|0\rangle$, where $|0\rangle$ is the ground state wave function and $|X\rangle$ denotes the state with displacement X . In the adiabatic limit $\omega_0=0$, the phonon degrees of freedom are described by classical variables, and no quantum fluctuations are present. The solution of the model involves a minimization of the electronic ground state as a function of X . As a result, the probability distribution is a single (or a few) δ function, centered at the values that minimize the energy. More explicitly, if the system is not polaronic, a single value of X minimizes the energy, while in the polaronic regime, two different minima are obtained. The polaron crossover is then associated with the coupling value in which a single δ function leaves place to two symmetric peaks. As soon as the quantum fluctuations of the lattice are restored by introducing a finite phonon frequency ω_0 , the δ functions broaden, but the qualitative features do not change. The polaronic regime is characterized by a *bimodal* distribution, while the nonpolaronic state present a *unimodal* distribution. In the particular case of a single particle on two sites, the polaronic regime presents two symmetric peaks at $X = \pm X_0$, and the nonpolaronic state in nondistorted, so that $P(X)$ is peaked at $X=0$.

Figure 1 shows the evolution of $P(X)$ varying λ in the two-site Holstein model for $\omega_0/t=0.1$ (representative of the adiabatic regime) and $\omega_0/t=4$ (representative of the antiadiabatic regime). In both cases a smooth crossover occurs between a quasifree electron state (unimodal distribution) and a polaronic state (bimodal distribution). The figure also clearly shows that the crossover is indeed much sharper in the adiabatic case than in the antiadiabatic one. Furthermore,

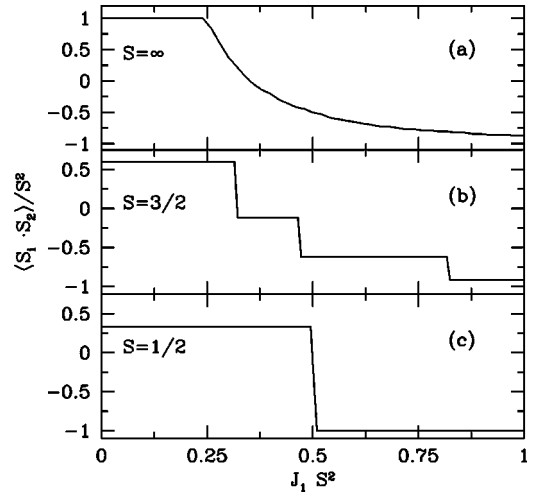


FIG. 2. $\langle \mathbf{S}_1 \cdot \mathbf{S}_1 \rangle$ for $S=\infty, 3/2, 1/2$ (from top to bottom) as a function of J_1 .

$P(X=0)$ in the polaronic region rapidly vanishes soon after the crossover in the adiabatic case, while it stays finite in the antiadiabatic, despite it is a local minimum in both cases. It is worth emphasizing that the monomodal to bimodal crossover of $P(X)$ has also been reported as signature to a crossover toward a “polaronic” state also in studies of the Holstein model *in the thermodynamic limit* using dynamical mean field theory (DMFT).^{22,23}

B. Magnetic correlations

In this section we discuss the behavior of the magnetic correlations in the two-site double exchange model. As mentioned above, we are only able to describe short range correlations. We parametrize the magnetic correlations between the two sites by means of the scalar product $\langle \mathbf{S}_1 \cdot \mathbf{S}_2 \rangle$ between the core spins.

Since our interest in the model is motivated by the manganites, we will always assume that J_H is the largest energy scale. In the $S=\infty$ case we let J_H go to infinity, and in the finite spin case, we take $J_H=10t$.

In the absence of electron-phonon coupling, and assuming that J_H is the largest energy scale, the direct antiferromagnetic exchange between the core electrons determines the magnetic properties of the system. For zero and small J_1 , the spins are ferromagnetically aligned due to the Hund’s coupling. Increasing J_1 , antiferromagnetic correlations tend to appear.

The nature of the spin correlations depends crucially on the value of the spin $S=S_1=S_2$, since the latter rules the possible values of $\langle \mathbf{S}_1 \cdot \mathbf{S}_2 \rangle$. More explicitly, in the classical spin case $\langle \mathbf{S}_1 \cdot \mathbf{S}_2 \rangle = S^2 \cos(\theta)$, where the canting angle θ between the spins is a continuous variable. The ferromagnet continuously evolves into a canted state as J_1 is enhanced. The canting angle asymptotically tends to π , corresponding to the antiferromagnetic state, as J_1 is enhanced. Panel (a) in Fig. 2 displays the dependence of $\langle \mathbf{S}_1 \cdot \mathbf{S}_2 \rangle$ on $J_1 S^2$ for the classical spin case for $J_H=\infty$.

In the quantum case the nonlocal magnetic correlation is given by

$$\langle \mathbf{S}_1 \cdot \mathbf{S}_2 \rangle = \frac{1}{2} [S_{\text{tot}}(S_{\text{tot}} + 1) - S_1(S_1 + 1) - S_2(S_2 + 1)], \quad (7)$$

and assumes only a few values. In Eq. (7) S_{tot} is the modulus of the total spin. For $S_1 = S_2 = 1/2$, $S_{\text{tot}} = 0$ and 1 are the two only possible values. For $S_1 = S_2 = 3/2$, we can have four values ($S_{\text{tot}} = 0, 1, 2, 3$). It must be noted anyway, that the total spin operator S^2 does not commute with the Hamiltonian (1), so that the energy eigenstates have no reason to be eigenstates of S_{tot}^2 .

An inspection to the results in the absence of electron-phonon coupling shows indeed that, for $S = 1/2$, the magnetic state abruptly varies, for $J_1 = J_1(\text{FE} - \text{AF})$, from a *fully polarized* ferromagnet to an antiferromagnetic state, which is not fully polarized. The “transition” is a level crossing between two states with different symmetry. The exact value of $\langle \mathbf{S}_1 \cdot \mathbf{S}_2 \rangle$ in this state depends on both J_H and J_1 , even if the dependence on J_1 [for $J_1 > J_1(\text{FE} - \text{AF})$] is really weak, as it appears in panel (c) of Fig. 2.

The $S = 3/2$ case is strictly analogous to $S = 1/2$, and shows the fully polarized FE state, followed by three different combinations of the AF states. Also in this case, the precise values of $\langle \mathbf{S}_1 \cdot \mathbf{S}_2 \rangle$ in the three states depend on J_H and J_1 , and the dependence on J_1 is really weak in each region. Moreover, the state with the largest negative correlation is really close to the full antiferromagnet. We label the two intermediate spin phases as canted 1 (CA1) and canted 2 (CA2), and the “most antiferromagnetic” as antiferromagnetic *tout court*. The dependence of $\langle \mathbf{S}_1 \cdot \mathbf{S}_2 \rangle$ on J_1 is shown in Fig. 2(b). We notice that the scale of J_1 associated with the change in the magnetic structure is consistent with the experimental estimates.²⁴

C. The phase diagram

In this section we discuss the interplay between the magnetic properties and the e -ph coupling and finally determine the phase diagram of our model. We tune the relevance of lattice and magnetic degrees of freedom, by varying the strength of the electron-phonon coupling λ , and of the antiferromagnetic coupling between the core spins J_1 . Then we draw various phase diagrams in the λ - J_1 plane. Each of the diagrams is characterized by the values of the spin S and of the phonon frequency ω_0 , that parametrize the relevance of quantum spin and lattice fluctuations, respectively. We consider the $S = \infty$, $S = 3/2$ and $S = 1/2$ cases, and $\omega_0/t = 0.1$ (adiabatic regime) and 4 (antiadiabatic regime). Finally, we always assume that the Hund’s rule coupling J_H is the largest energy scale. In the classical case, we take $J_H = \infty$, and in the quantum cases, we use $J_H = 10t$. We denote “discontinuous transitions” with full lines and “continuous transitions” with dashed lines.

1. The effect of J_1 on the polaron crossover

In Sec. III A, we have briefly described the conditions ruling the polaron crossover in the Holstein model. In the adiabatic regime $\omega_0/t \ll 1$, the condition for a polaron ground state is that the polaron binding energy $E_{\text{pol}} = g^2/\omega_0$

is larger than the free electron kinetic energy, measured by t . It is quite natural to generalize this condition to the double-exchange model, at least when the polaron crossover occurs between two phases that share a common magnetic state. In this case, we can replace the bare hopping t by the “magnetically renormalized” kinetic energy at $\lambda = 0$ (\bar{t}). Thus the crossover condition is determined by the condition

$$\lambda_{mg} = \frac{g^2}{\omega_0 \bar{t}} \simeq 1. \quad (8)$$

In the $S = \infty$ case the magnetic hopping is given by

$$\bar{t} = t \cos\left(\frac{\theta}{2}\right), \quad (9)$$

where θ is the canting angle between the t_{2g} spins.^{2,3} In the quantum cases $S = 1/2$ and $S = 3/2$, one can view the canting angle as a quantized quantity, that can assume only a few discrete values. We anticipate that these are *not* the quantized values of the semiclassical approximation.

Regardless the value of S and ω_0/t , for small values of J_1 the ground state is always ferromagnetic due to the Hund’s rule. A crossover occurs between a ferromagnetic itinerant electron and a ferromagnetic polaron. Within this region, the magnetic hopping is fixed to the free value $\bar{t} \equiv t$, and does not depend on J_1 . As a result, the model is completely equivalent to a two-site Holstein model, and the crossover is associated with a vertical line in the λ - J_1 diagram, as shown in all the phase diagrams (Figs. 3–8). The crossover value of λ depends only on the ratio ω_0/t , and moves from the $\lambda \simeq 1$ in the extreme adiabatic limit, to $\lambda \simeq 1.2$ for $\omega_0/t = 0.1$, to a substantially larger value ($\lambda \simeq 3.46$) for $\omega_0/t = 4$, where the condition for the polaron crossover is close to $\alpha^2 \simeq 1$ (that implies $\lambda \simeq 4$).

Increasing J_1 , phases with antiferromagnetic correlation between the core spins appear. The nature of these phases depends on the value of S , as shown in Sec. III B. We start from the quantum cases, that present sharp level crossings at $\lambda = 0$, where \bar{t} sharply jumps following the magnetic correlations shown in Fig. 2. If we neglect the really weak dependence on J_1 of $\langle \mathbf{S}_1 \cdot \mathbf{S}_2 \rangle$ *within* a given magnetic phase, the

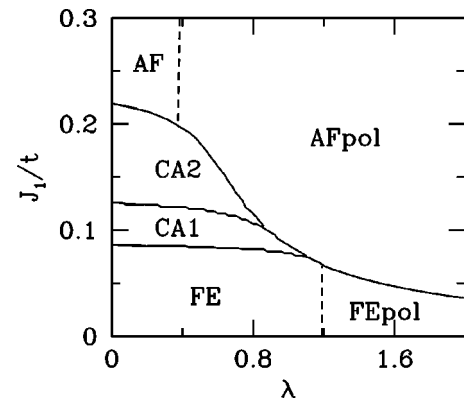
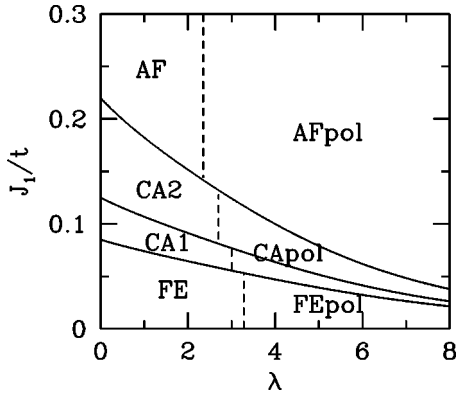
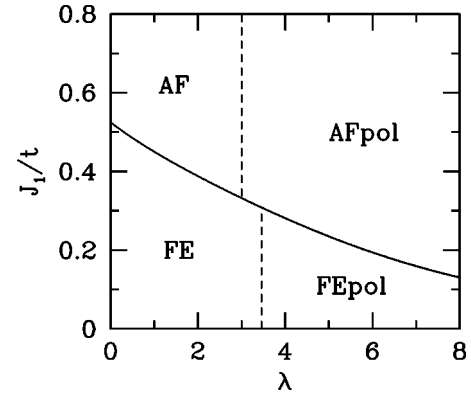


FIG. 3. Phase diagram for $S = 3/2$ and $\omega_0/t = 0.1$.


 FIG. 4. Phase diagram for $S=3/2$ and $\omega_0/t=4$.

 FIG. 6. Phase diagram for $S=1/2$ and $\omega_0/t=4$.

polaron crossover is controlled by the condition (8), where \bar{t} is the value corresponding to the actual magnetic phase.

The exact results obtained as described in Sec. II confirm this expectation, and the polaron crossovers among phases with the same magnetic correlation are in fact delimited by vertical dashed lines in all the diagrams for $S=1/2$ and $S=3/2$ (Figs. 3–6). The value of the crossover coupling obviously changes in the different magnetic phases. The FE state is the one with the largest kinetic energy due to the double exchange mechanism, so that the critical λ is the highest in this phase, and it decreases by decreasing the value of the magnetic correlation according to Eq. (8) (see, e.g., Figs. 3,4). Notice that the effect of the value of $\langle \mathbf{S}_1 \cdot \mathbf{S}_2 \rangle$ on the crossover coupling is much more evident in the adiabatic limit (Fig. 3), where the competition between the polaron energy and the kinetic energy rules the crossover, than in the antiadiabatic regime (Fig. 4), where the electronic kinetic energy is not the most relevant quantity. In the extreme antiadiabatic limit $\omega_0/t \rightarrow \infty$ this dependence must completely disappear, since the kinetic energy plays no role in the crossover.

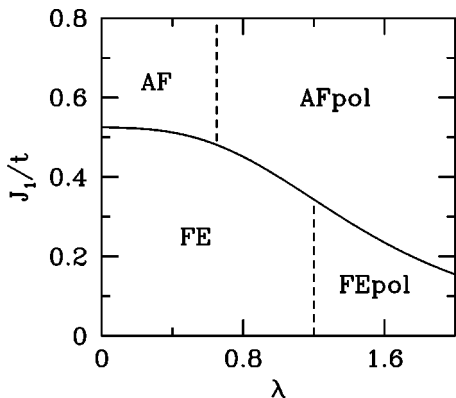
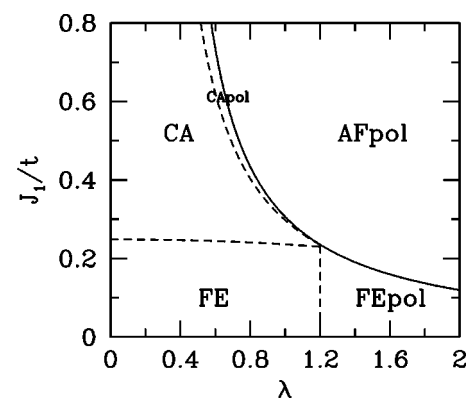
The formation of polaron does not only occur as smooth crossover between states with the same magnetic correlation. Indeed, in the $S=1/2$ case (see Fig. 5), if we continuously increase J_1 , we have that, between the vertical dashed lines corresponding to the polaronic crossovers within the FE and the AF phases, a first-order “transition” (level crossing) occurs from a ferromagnetic non-polaronic state and an antifer-

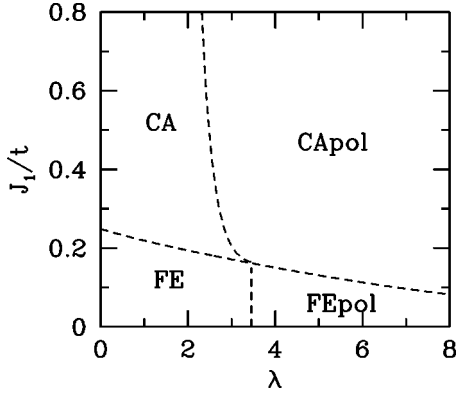
romagnetic polaron. The interplay between the localizing effect of both the e -ph and the antiferromagnetic magnetic interaction strongly favors the AF polaronic state with respect to the competing phases.

Similar level crossings occur for all the finite-spin cases, with more involved details depending upon the value of S and ω_0 . For example, in the antiadiabatic regime $\omega_0/t=4$, the FE-AF polaron “transition” occurs only in a narrow range of parameters (see Fig. 6, compared to the adiabatic case, Fig. 5). This is simply due to the fact that, in this regime, the crossover values for λ in the FE and the AF are very close. In the extreme antiadiabatic limit $\omega_0/t \rightarrow \infty$ this region would indeed vanish.

In the richer $S=3/2$ case, the CA1 and CA2 states intrude between the FE and the AF at weak e -ph coupling. In the adiabatic regime (see Fig. 3), no polaron crossover occurs within the canted phases, and both these phases undergo a first order “transition” to the AF polaron. Only the FE and AF phases display the usual polaron crossover. In the antiadiabatic case, besides the aforementioned reduction of the regions in which the polaron formation becomes first order, canted polaronic states are stabilized by the phonon quantum fluctuations. (The “critical” frequency above which canted polaronic states appear is $\omega_0/t \approx 1$).

In the $S=\infty$ case, where canted phases with a continuous canting angle are stable, the polaron crossover is not represented by a vertical line, since the kinetic energy is a continuous function of J_1 with $\bar{t}=t \cos \theta(\bar{J}_1)$, and $\theta(\bar{J}_1)$ is the


 FIG. 5. Phase diagram for $S=1/2$ and $\omega_0/t=0.1$.

 FIG. 7. Phase diagram for $S=\infty$ and $\omega_0/t=0.1$.

FIG. 8. Phase diagram for $S=\infty$ and $\omega_0/t=4$.

value of the canting angle at $\lambda=0$. Again, all results are consistent with the condition (8). In this case, the phonon fluctuations play a somewhat qualitative role. In the extreme adiabatic limit the CA state undergoes a level crossing to the AF polaronic state. The e -ph interaction and the antiferromagnetic coupling J_1 cooperate to stabilize the AF polaron without forming a canted polaron. As soon as we introduce a finite, but small ω_0/t , a tiny slice of a canted polaronic phase appears to bridge between the canted state and the antiferromagnetic polaron. In the antiadiabatic regime, the huge quantum fluctuations strongly favor a canted polaronic state, and the antiferromagnetic polaron appears only for $\lambda > 10$ and $J_1 > 2$.

The above results show that the effect of the magnetic correlations on the small polaron crossover is influenced by the spin quantum fluctuations. In particular, the $S=3/2$ case, which is relevant to the manganites is not qualitatively similar to the classical spin case, that is usually considered for simplicity. Many features of the $S=3/2$ case are in fact direct consequences of the quantum nature of the spins, and are similar to the simplest quantum case $S=1/2$.

2. The effect of e -ph coupling on magnetic “transitions”

In this section we analyze how the various magnetic “transitions” described in Sec. III B are influenced by the e -ph interaction. In the previous section we have found analytical results for the “transition” from FE to AF states for $J_H \rightarrow \infty$. The expressions, given by Eqs. (5) and (6), can be recast in the common form

$$J_1^c S^2 = \frac{E_H(\text{AF}) - E_H(\text{FE})}{\frac{\langle \mathbf{S}_1 \cdot \mathbf{S}_2 \rangle_{\text{FE}}}{S^2} - \frac{\langle \mathbf{S}_1 \cdot \mathbf{S}_2 \rangle_{\text{AF}}}{S^2}}, \quad (10)$$

where $E_H(\text{AF})$ [$E_H(\text{FE})$] is the energy of the Holstein model for the antiferromagnetic (ferromagnetic) spin alignment, and $\langle \mathbf{S}_1 \cdot \mathbf{S}_2 \rangle$ in the different magnetic phases is computed at $g=0$. In particular, the evaluation of E_H for a given phase simply amounts to finding the ground state of the Holstein model where the bare hopping t is replaced by \bar{t} . This rela-

tion also holds for the case of $S=3/2$, once the proper value for the kinetic energy in the antiferromagnetic phase $\bar{t}=t/4$ is used.

Equation (10) results from the competition between the magnetic energy balance, controlled by J_1 , and the “polaronic” energy, i.e., the energy resulting from the e -ph coupling. Since the AF phase has always a smaller hopping with respect to the FE phase, the first qualitative effect of the e -ph interaction is to lower the energy of the antiferromagnetic phase with respect to the ferromagnetic one, therefore favoring antiferromagnetism. The region of stability of the FE phase is always shrunk by increasing λ . More generally, the e -ph interaction favors phases with smaller values of $\langle \mathbf{S}_1 \cdot \mathbf{S}_2 \rangle$, so that the boundaries of the different magnetic phases are always marked by downward curves in the J_1 - λ plane.

In the limit of small t , the energy difference in the numerator of Eq. (10) reduces to the pure kinetic energy of the Holstein model close to the atomic limit. Defining $\gamma = \bar{t}/t$, we can write

$$\begin{aligned} \lim_{t \rightarrow 0} [E_H(\gamma t) - E_H(t)] &= \lim_{t \rightarrow 0} (1 - \gamma) t \frac{E_H[t + (1 - \gamma)t] - E_H(t)}{(1 - \gamma)t} \\ &= (1 - \gamma) t \frac{\partial E_H(t)}{\partial t} = -E_H^{\text{kin}}(1 - \gamma). \end{aligned} \quad (11)$$

In the small t limit the condition (10) reduces then to

$$J_1^c = \kappa(S)(-E_H^{\text{kin}}), \quad (12)$$

where $\kappa(S)$ is a constant that contains the factor $1 - \gamma$, and depends on the value of the spin S and on the “transition” under consideration, such that, in the absence of e -ph interaction the condition is simply $J_1^c = \kappa(S)t$. This latter relation is analogous to Eq. (8), since the effect of the e -ph interaction results in the substitution $t \rightarrow -E_H^{\text{kin}}$, but, contrary to that, it is valid only for $t \rightarrow 0$.

This result gives valuable information about the role of the retardation effects in the e -ph coupling. In general terms, the interaction mediated by the phonons is in fact retarded, and becomes instantaneous only if $\omega_0/t \rightarrow \infty$. In such a limit, as we have shown, the kinetic energy rules the magnetic “transitions.” As soon as the approximation $t \rightarrow 0$ is released, the retardation effects imply that Eq. (10) must be used. Notice that $E_H(\text{AF}) - E_H(\text{FE}) = -E_H^{\text{kin}} + \Delta$, where Δ is the difference between the e -ph interaction energies in the two phases, and turns out to be always positive. The overall effect of the retarded e -ph interaction is therefore to reduce the stability of FE phases with respect to AF and CA phases.

In the $S=3/2$ case all the magnetic “transitions” are discontinuous, as described in Sec. III B, so that similar arguments can be applied, and Eq. (10) allows one to compute the “transition” coupling, once the energy of the Holstein model and the magnetic energy of the appropriate phases are known.

The situation is different only for the continuous transition n between the FE and CA phases in the classical spin

case. In this case the continuity of the “transition” implies that the energy difference between the phases is infinitesimal, so that $E_H^{\text{kin}} = -t \partial E_H(t) / \partial t$ rules the “transition” not only for small t , but for arbitrary values of t , as shown by Eq. (4). This preliminary analysis suggests a really important difference between the classical spin limit $S = \infty$ and the quantum $S = 3/2$ case.

Now we can give some description and interpretation of the exact phase diagrams in light of the above analysis. In the adiabatic limit $\omega_0/t = 0$, for finite value of S , and for $\lambda < \lambda_{\text{pol}}$, the energy of the e -ph model alone does not depend upon λ , so that the relative stability of the various magnetic phases is in turn expected to be λ independent. The magnetic “transitions” are therefore associated with horizontal lines in the λ - J_1 plane. If we introduce phonon fluctuations, the kinetic energy depends upon λ also before the crossover, and the boundary between the magnetic states acquires a finite slope, that becomes larger and larger by increasing ω_0/t . This behavior can be easily seen comparing Fig. 3 with 4 (or Fig. 5 with 6). The case of the classical spin variables, where the magnetization is a continuous variable, can be understood in similar terms. The crossover between the FE and the CA phase in fact closely follows the curve obtained using Eq. (4).

As discussed previously, the phonon fluctuations always favor FE phases with respect to AF and CA phases, as it can be seen comparing the phase diagrams for $\omega_0/t = 0.1$ with the corresponding with $\omega_0/t = 4$ (at the same value of λ). In we increase the quantum fluctuations of the phonons, by increasing the phonon frequency ω_0 , the retardation effects are decreased, so that the localization of the electrons is made more difficult. An enhanced mobility of the electron results in an enhanced stability of the FE phases due to the double exchange mechanism.

IV. RELEVANCE OF THE TWO-SITE SYSTEM

In this section we discuss the relationship between the two-site model and larger systems. Some peculiarities of the two-site system must be addressed in order to properly compare our findings with those of larger systems. We notice that, in the absence of magnetic interactions (Holstein model), the lattice deformations obtained within the present model (Fig. 1) are similar to those of an half-filled band.²³ We can therefore compare the polaron crossover obtained through the procedure outlined in Sec. III A with a spinless fermion system with $x = 1/2$ or, in the presence of magnetic interaction, with the case of one polaron every two sites. However the spectral functions (see Appendix A) are similar to those obtained for a single polaron in an infinite size lattice.¹⁷

We emphasize that the capability of the two-site system to capture the physics of polaron crossover is not accidental and can be easily rationalized. This is essentially due to the extreme short-range character of the polaronic state. In this spirit we expect the results of our calculations to be somehow related to a dynamical mean field theory, where the local quantum fluctuations are exactly taken into account, while the spatial correlations are frozen.²⁵ Similarly to the

DMFT, our exact solutions faithfully reproduce the physics of the model if the local and short-range effects are dominant, as it is the case for the manganites. More specifically the one-electron solution of the two-site Holstein model (see Appendix A) is surprisingly similar to the one-electron solution of the Holstein model for an infinite lattice within DMFT. Looking at a given site, the role played by the “effective quantum medium” of DMFT is here simply played by the other site. It must be noticed, however, that our small cluster cannot determine whether the polaronic and the delocalized states are Fermi liquids or not.

To check whether the above considerations about the relevance of the two-site cluster as far as the polaron crossover is concerned may be valid also in the presence of magnetic interaction, we compare our results to more realistic models for manganites. There are not indeed so many solutions of the double exchange model in the presence of e -ph coupling. In particular, to the best of our knowledge, there are no phase diagrams studies of the Holstein-double-exchange model. Studies of more realistic JT double-exchange model, keeping into account the full tridimensional structure and the orbital degrees of freedom, are instead available, but most of them are forced to consider the classical limit for either the phonons or the core spins, due to the large local Hilbert space.^{15,26,27,20}

Among the various studies we want to draw the attention of the reader to Refs. 15 and 26, in which phase diagrams of, respectively, $x = 0$ and $x = 0.5$ $\text{La}_{1-x}\text{Ca}_x\text{MnO}_3$, in agreement with experimental findings are reported. A common feature of the above works is the presence of a transition at small values of J_1 and intermediate λ from an itinerant FE phase to a FE phase with significant lattice distortions, labeled as JT phase in Ref. 15, and orbitally ordered state in Ref. 26. This transition represents the natural counterpart of the polaron crossover within the FE phase that we find in our model, as it can be seen by direct comparison with all our phase diagrams. Despite the density of carriers is different in the two studies, the e -ph coupling for which this transition occurs is very similar. In the same references it is also found that finite-size effects are not so important for the description of this transition, thus confirming that the physics underlying the polaron crossover is essentially local.

Other analogies between phases diagram of Refs. 15 and 26 and Fig. 7 can be noticed. In all the phase diagrams, increasing J_1 , the FE phase is replaced by some other magnetic ordering (“non-FE” phases). In our model the ferromagnet is simply replaced by CA or AF phases, while in the more realistic models, more complicated phases involving orbital degrees of freedom are stabilized (the CE phase for $x = 0.5$ and the A-type antiferromagnet for $x = 0$). Nonetheless, the shape of the curves separating the FE phase to the “non-FE” phases looks very similar in all the systems, despite the different nature of the “non-FE” phase in the different models. We emphasize that our simple model is not able to account for the different orbital and magnetic orderings found by experiments, while the more realistic JT coupling correctly reproduces the experimentally observed phases.

V. CONCLUSIONS

In this work the two-site double exchange model for an electron coupled with phonons is solved exactly for an extremely wide range of parameters and physical regimes. For $S=1/2$ and $S=\infty$ we give an analytical exact solution for arbitrary e -ph coupling and phonon frequency. For $S=3/2$ the solution is obtained through standard numerical techniques. The availability of these solutions allows us to study the effect of both phonon and spin quantum fluctuations, and of their mutual interplay.

This study, though limited to the extreme small size of the two-site cluster, is shown to be a good description of larger systems, since the relevant physics involves local and short-ranged quantities. One of our main results is a complete characterization of the effect of the double exchange and of an antiferromagnetic coupling between the t_{2g} spins on the small polaron crossover. In this regard, we give an analytical estimate for the crossover coupling, given by $\lambda_{mg} = g^2/\omega_0\bar{t} \simeq 1$, where \bar{t} is the kinetic energy renormalized by the magnetic effects.

From a complementary point of view, we considered in detail the effect of the e -ph interaction on the magnetic properties of the system. In this case, we give an analytical condition for the magnetic ‘‘transitions’’ in the presence of a finite λ , given by Eq. (10). This relation can be simplified in the limit $t \rightarrow 0$, where there is no retardation effect. The comparison between the general case and the atomic limit allows us to quantitatively describe the role of retardation in stabilizing AF (or CA) phases.

A comparison of the realistic $S=3/2$ case with the classical spin case $S=\infty$ shows that this latter approximation does not reproduce some qualitative features of the phase diagram. A proper study of the manganites should therefore take into account the quantum nature of the core spins.

ACKNOWLEDGMENTS

We acknowledge useful discussions with D. Feinberg and C. Castellano.

APPENDIX A: THE EXACT SOLUTION OF THE TWO-SITE HOLSTEIN MODEL

In this appendix we sketch the solution through a continued fraction expansion of the two-site Holstein model. A continued fraction solution has been already reported in the literature²⁸ for a related model in the field of quantum optics. Here we derive the continued fraction expansion for eigenvalues and eigenvectors of the two-site Holstein model using a different method.

The Holstein model for an electron on two sites can be written in a pseudospin representation in terms of the Pauli matrices

$$H_H = \omega_0 \mathbf{1} a^\dagger a - g \sigma_z (a + a^\dagger) - t \sigma_x, \quad (\text{A1})$$

where $\mathbf{1}$ is the unity matrix. The Hamiltonian can be diagonalized in the electron subspace using a transformation introduced in Ref. 8

$$U = \frac{1}{\sqrt{2}} \begin{pmatrix} 1 & (-)^{a^\dagger a} \\ -1 & (-)^{a^\dagger a} \end{pmatrix} \quad (\text{A2})$$

and the property

$$(-)^{a^\dagger a} (a + a^\dagger) (-)^{a^\dagger a} = -(a + a^\dagger) \quad (\text{A3})$$

we obtain for $\tilde{H}_H = U H_H U^{-1}$

$$\tilde{H}_H = \begin{pmatrix} \tilde{H}_H(t) & 0 \\ 0 & \tilde{H}_H(-t) \end{pmatrix}, \quad (\text{A4})$$

where

$$\tilde{H}_H(\pm t) = \omega_0 a^\dagger a - g(a + a^\dagger) \mp t (-)^{a^\dagger a}. \quad (\text{A5})$$

In each block we have a purely phononic Hamiltonian $\tilde{H}_H(\pm t)$. The eigenvalues and eigenvectors can be determined by continued fraction solution for the resolvent between $|m\rangle$ and $|n\rangle$ phonon states

$$G_{m,n}^\pm(\omega) = \left\langle m \left| \frac{1}{\omega - \tilde{H}_H(\pm t)} \right| n \right\rangle. \quad (\text{A6})$$

Using

$$\frac{1}{\omega - H} = \frac{1}{\omega - H_0} + \frac{1}{\omega - H_0} H_I \frac{1}{\omega - H} \quad (\text{A7})$$

with $H_0 = \omega_0 a^\dagger a \mp t (-)^{a^\dagger a}$ and $H_I = -g(a + a^\dagger)$ we get the recursion

$$G_{m,n}^\pm(\omega) = \delta_{m,n} G_0^\pm(\omega - n\omega_0) - g \sum_p G_0^\pm(\omega - n\omega_0) X_{n,p} G_{p,n}^\pm(\omega), \quad (\text{A8})$$

where $X_{n,p} = \langle n | a + a^\dagger | p \rangle$. This tridiagonal recursion can be solved for the diagonal elements through a continued fraction solution²⁹

$$G_{n,n}^\pm(\omega) = \frac{1}{\omega - n\omega_0 \pm t - \Sigma_{em} - \Sigma_{abs}}, \quad (\text{A9})$$

where

$$\Sigma_{abs} = \frac{ng^2}{\omega + \omega_0 \mp t - \frac{(n-1)g^2}{\omega + 2\omega_0 \pm t - \frac{(n-2)g^2}{\omega + n\omega_0 + (\mp)^n t}}}} \quad (\text{A10})$$

and

$$\Sigma_{em} = \frac{(n+1)g^2}{\omega - \omega_0 \mp t - \frac{(n+2)g^2}{\omega - 2\omega_0 \pm t - \frac{(n+3)g^2}{\omega - n\omega_0 \mp t - \dots}}}. \quad (\text{A11})$$

At zero temperature the Green function of the two-site Holstein model defined as

$$G_{i,j}(\omega) = -i \langle 0 | T c_i(t) c_j^\dagger(0) | 0 \rangle \quad (\text{A12})$$

can be expressed as

$$G_{1,1}(\omega) = \frac{1}{2} [G_{0,0}^+(\omega) + G_{0,0}^-(\omega)],$$

$$G_{1,2}(\omega) = \frac{1}{2} [G_{0,0}^+(\omega) - G_{0,0}^-(\omega)], \quad (\text{A13})$$

therefore $G_{0,0}^\pm$ are the k -space propagators whose poles determine the bonding and antibonding eigenvalues of H_H . The residues of the lowest energy pole of $G_{n,n}^\pm$ determine the square of the projection of the phonon ground state on the $|m\rangle$ state b_m^\pm . Let us write Eq. (A11) for $n=0$ in a recursive fashion

$$\Sigma_p^\pm = \frac{pg^2}{\omega - p\omega_0 + (\mp)^p t - \Sigma_{p+1}^\pm}, \quad (\text{A14})$$

where Σ_1^\pm is the continued fraction of Eq. (A11) therefore the equation which gives the eigenvalue of the two-site Holstein model is

$$\omega \pm t - \Sigma_1^\pm = 0. \quad (\text{A15})$$

By linearizing this recursion around the m th solution E_m of Eq. (A15) letting $z_p^\pm = \partial \Sigma_p^\pm / \partial E_m$ we get

$$z_p^\pm = (z_{p+1}^\pm - 1) \frac{pg^2}{E_m - p\omega_0 + (\mp)^p t - \Sigma_{p+1}^\pm}. \quad (\text{A16})$$

Finally the coefficient b_m^\pm is given by

$$b_m^\pm = \sqrt{\frac{1}{1 - z_1^\pm}}. \quad (\text{A17})$$

The (quantum) probability distribution function for the displacement operator can be determined using the harmonic oscillator wave functions $\Psi_n(X)$ as

$$P(X) = \sum_{m,n} [(b_m^+)^* b_n^+ + (b_m^-)^* b_n^-] \Psi_m^*(X) \Psi_n(X). \quad (\text{A18})$$

APPENDIX B: THE EXACT SOLUTION OF THE TWO-SITE HOLSTEIN DOUBLE-EXCHANGE MODEL FOR $S=1/2$

Let us start from the case $g=0$. We choose the following basis set labeling the states according to the total spin $S_{\text{tot}} = S + s$ where S is the spin of the Mg^{3+} ion and s that of the e_g electron. We have two states in the $S=3/2$ sector $|A\rangle = |\uparrow\uparrow\uparrow\rangle|\uparrow\cdot\rangle, |A'\rangle = |\uparrow\uparrow\uparrow\rangle|\cdot\uparrow\rangle$ and six states in the $S=1/2$ sector $|B\rangle = |\uparrow\uparrow\downarrow\rangle|\uparrow\cdot\rangle, |B'\rangle = |\uparrow\uparrow\downarrow\rangle|\cdot\uparrow\rangle, |C\rangle = |\uparrow\downarrow\uparrow\rangle|\uparrow\cdot\rangle, |C'\rangle = |\uparrow\downarrow\uparrow\rangle|\cdot\uparrow\rangle, |D\rangle = |\uparrow\uparrow\uparrow\rangle|\downarrow\cdot\rangle, |D'\rangle = |\uparrow\uparrow\uparrow\rangle|\cdot\downarrow\rangle$, where $|\uparrow\rangle$ ($|\downarrow\rangle$) represent an up (down) spin state for the core spins and $|\uparrow\rangle$ ($|\downarrow\rangle$) are the same for the e_g electrons. The Hamiltonian is invariant for flipping of all the spins so these are all the states we need. The states $|A\rangle$ and $|D\rangle$ have a FE character while the states $|B\rangle$ and $|C\rangle$ have AF character. The $S=3/2$ subspace, spanned by the combinations of $|A\rangle$ and $|A'\rangle$, decouples from the other states even in the presence of e -ph phonon interaction.

If we consider the symmetric and antisymmetric combinations

$$|A^\pm\rangle = \frac{1}{\sqrt{2}}(|A\rangle \pm |A'\rangle),$$

$$|B^\pm\rangle = \frac{1}{\sqrt{2}}(|B\rangle \pm |B'\rangle),$$

$$|C^\pm\rangle = \frac{1}{\sqrt{2}}(|C\rangle \pm |C'\rangle),$$

$$|D^\pm\rangle = \frac{1}{\sqrt{2}}(|D\rangle \pm |D'\rangle), \quad (\text{B1})$$

in the absence of the e -ph interaction the symmetric and antisymmetric sectors are decoupled so that the part of the Hamiltonian matrix which pertains to Hund and antiferromagnetic interactions consists of three blocks:

$$H_{3/2} = \begin{pmatrix} \frac{J_1 - J_H}{4} - t & 0 \\ 0 & \frac{J_1 - J_H}{4} + t \end{pmatrix}, \quad (\text{B2})$$

$$H_{1/2,+} = \begin{pmatrix} -\frac{J_1 + J_H}{4} & \frac{J_1}{2} - t & 0 \\ \frac{J_1}{2} - t & -\frac{J_1 - J_H}{4} & -\frac{J_H}{2} \\ 0 & -\frac{J_H}{2} & \frac{J_1 + J_H}{4} - t \end{pmatrix} \quad (\text{B3})$$

the last block $H_{1/2,-}$ can be obtained from Eq. (B3) by the substitution $t \rightarrow -t$. The e -ph matrix elements couple the subspaces (A^+, B^+, C^+, D^+) and (A^-, B^-, C^-, D^-) . The subspace spanned by $|A^\pm\rangle$ can be diagonalized independently having the same eigenvalues and eigenvectors of a

two-site Holstein model (see Appendix A). The Hamiltonian matrix in the $S_{1/2}$ can be written

$$H_{1/2} = \begin{pmatrix} H_{1/2,+} + \omega_0 \mathbf{1} a^\dagger a & -g \mathbf{1} (a^\dagger + a) \\ -g \mathbf{1} (a^\dagger + a) & H_{1/2,-} + \omega_0 \mathbf{1} a^\dagger a \end{pmatrix}. \quad (\text{B4})$$

Here $\mathbf{1}$ is the 3×3 unit matrix. We can diagonalize $H_{1/2}$ in the phonon space by means of the unitary transformation

$$\tilde{H}_{1/2} = \begin{pmatrix} [\omega_0 a^\dagger a - g(a^\dagger + a)] \mathbf{1} + H_{1/2}^{\text{at}} - t(-)^{a^\dagger a} \Delta & 0 \\ 0 & [\omega_0 a^\dagger a + g(a^\dagger + a)] \mathbf{1} + H_{1/2}^{\text{at}} + t(-)^{a^\dagger a} \Delta \end{pmatrix}, \quad (\text{B6})$$

where we have split $H_{1/2,\pm} = H_{1/2}^{\text{at}} \pm t \Delta$ in the atomic ($t=0$) part and in the hopping dependent term

$$\Delta = \begin{pmatrix} 0 & 1 & 0 \\ 1 & 0 & 0 \\ 0 & 0 & 1 \end{pmatrix} \quad (\text{B7})$$

and $H_{1/2}^{\text{at}}$ can be obtained from Eq. (B4) with $t=0$. The Hamiltonian Eq. (B6) can be diagonalized in each spin sector by an independent transformation which diagonalizes $H_{1/2,\pm}$ for a given phonon number n . The diagonalization gives six eigenvalues $E_{1/2,\pm}(n)$ for each phonon number. For $n=0$ and $J_H \gg t, J_1$ the lowest of them are

$$E_{1/2,-}^{\text{FE}} = -\frac{J_H}{4} - t + \frac{J_1}{4}, \quad (\text{B8})$$

$$U = \frac{1}{2} \begin{pmatrix} [1 + (-)^{a^\dagger a}] \mathbf{1} & [-1 + (-)^{a^\dagger a}] \mathbf{1} \\ [-1 + (-)^{a^\dagger a}] \mathbf{1} & [1 + (-)^{a^\dagger a}] \mathbf{1} \end{pmatrix}. \quad (\text{B5})$$

Using the property given in Eq. (A3) we get for $\tilde{H}_{1/2} = U H_{1/2} U^{-1}$

$$E_{1/2,-}^{\text{AF}} = -\frac{J_H}{4} - \frac{t}{2} - \frac{J_1}{2}. \quad (\text{B9})$$

By replacing $t \rightarrow t(-)^{a^\dagger a}$ we are left with a purely phononic Hamiltonian in the FE/AF sector

$$\tilde{H}_{1/2}^{\text{FE}} = \omega_0 a^\dagger a - g(a^\dagger + a) - \frac{J_H}{4} - t(-)^{a^\dagger a} + \frac{J_1}{4}, \quad (\text{B10})$$

$$\tilde{H}_{1/2}^{\text{AF}} = \omega_0 a^\dagger a - g(a^\dagger + a) - \frac{J_H}{4} - \frac{t}{2} (-)^{a^\dagger a} - \frac{J_1}{2}. \quad (\text{B11})$$

The comparison between the energies of the FE and the AF phases leads to the condition (6) for the magnetic “transition.”

-
- ¹C. Zener, Phys. Rev. **82**, 403 (1951).
²P.W. Anderson and H. Hasegawa, Phys. Rev. **100**, 675 (1955).
³P. G. de Gennes, Phys. Rev. **188**, 141 (1960).
⁴S. Jin, T.H. Tiefel, M. McCormack, F.A. Fastnacht, R. Ramesh, and L.H. Chen, Science **264**, 413 (1994).
⁵A. J. Millis, P. B. Littlewood, and B. I. Shraiman, Phys. Rev. Lett. **74**, 5144 (1995).
⁶G. Zhao, K. Conder, H. Keller, and K.A. Müller, Nature (London) **381**, 676 (1996); A. Lanzara, N.L. Saini, M. Brunelli, F. Natali, A. Bianconi, P.G. Radaelli, and S.-W. Cheong, Phys. Rev. Lett. **81**, 878 (1998); D. Louca, T. Egami, E.L. Brosha, H. Röder, and A.R. Bishop, Phys. Rev. B **56**, 8475 (1997); S.J.L. Billinge, R.G. DiFrancesco, G.H. Kwei, J.J. Neumeier, and J.D. Thompson, Phys. Rev. Lett. **77**, 715 (1996).
⁷T. Holstein, Ann. Phys. (N.Y.) **8**, 325 (1959).
⁸F. de Pasquale, S. Ciuchi, J. Bellissard, and D. Feinberg, *Reviews of Solid State Science* edited by A.K. Gupta, S.K. Joshi, and C.N.R. Rao (World Scientific, Singapore, 1988), Vol. 2, p. 443.
⁹D. Feinberg, S. Ciuchi, and F. de Pasquale, Int. J. Solid State B **4**, 1317 (1990).
¹⁰A.S. Alexandrov, V.V. Kabanov, and D.K. Ray, Phys. Rev. B **49**, 9915 (1994).
¹¹Yu.A. Firsov and E.K. Kudinov, Phys. Solid State **39**, 1930 (1997).
¹²J. Ranninger and U. Thibblin, Phys. Rev. B **45**, 7730 (1992).
¹³E.V.L. de Mello and J. Ranninger, Phys. Rev. B **55**, 14 872 (1997).
¹⁴M. Acquarone, J.R. Iglesias, M. A. Gusmão, C. Noce, and A. Romano, Phys. Rev. B **58**, 7626 (1998).
¹⁵T. Hotta, S. Yunoki, M. Mayr, and E. Dagotto, Phys. Rev. B **60**, 15 009 (1999).
¹⁶M. Capone, W. Stephan, and M. Grilli, Phys. Rev. B **56**, 4484 (1997).
¹⁷S. Ciuchi, F. de Pasquale, S. Fratini, and D. Feinberg, Phys. Rev. B **56**, 4494 (1997).
¹⁸M. Capone, S. Ciuchi, and C. Grimaldi, Europhys. Lett. **42**, 523 (1998).
¹⁹J. Chatterjee, M. Mitra, and A.N. Das, Eur. Phys. J. B **18**, 573 (2000).
²⁰D. Feinberg, P. Germain, M. Grilli, and G. Seibold, Phys. Rev. B **57**, 5583 (1998); M. Capone, D. Feinberg, and M. Grilli, Eur. Phys. J. B **17**, 103 (2000).
²¹Notice that Eq. (3) gives the approximate θ_{MLF} of Ref. 19 once the approximation $E_{\text{kin}} \approx -t \exp -\alpha^2$ valid in the extreme antiadiabatic regime has been made.

- ²²J.K. Freericks, M. Jarrell, and D.J. Scalapino, Phys. Rev. B **48**, 6302 (1993).
- ²³A.J. Millis, R. Mueller, and B.I. Shraiman, Phys. Rev. B **54**, 5389 (1996).
- ²⁴T.G. Perring *et al.* Phys. Rev. Lett. **78**, 3197 (1997).
- ²⁵A. Georges, G. Kotliar, W. Krauth, and M. Rozenberg, Rev. Mod. Phys. **68**, 13 (1996).
- ²⁶S. Yunoki, T. Hotta, and E. Dagotto, Phys. Rev. Lett. **84**, 3714 (2000).
- ²⁷S. Fratini, D. Feinberg, and M. Grilli, Eur. Phys. J. B **22**, 157 (2001).
- ²⁸S. Swain, J. Phys. A **6**, 192 (1973).
- ²⁹V.S. Viswanath and G. Müller, *The Recursion Method* (Springer-Verlag, Berlin, 1994).